# Scaling Relations from Gamma Ray Bursts to constrain Cosmography

*Salvatore Capozziello*

*Università di Napoli " Federico II "*
*and*
*INFN sez. di Napoli*

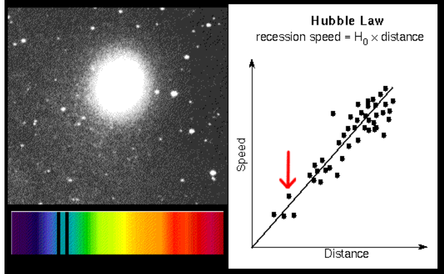


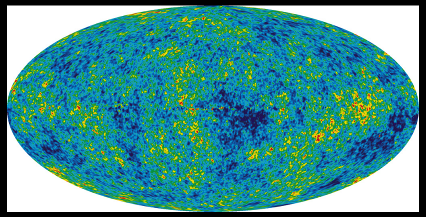

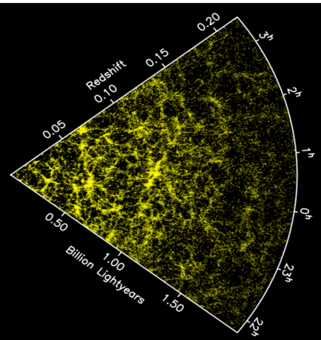


*All observational cosmology tests agree: ~96% of the Universe is dark*

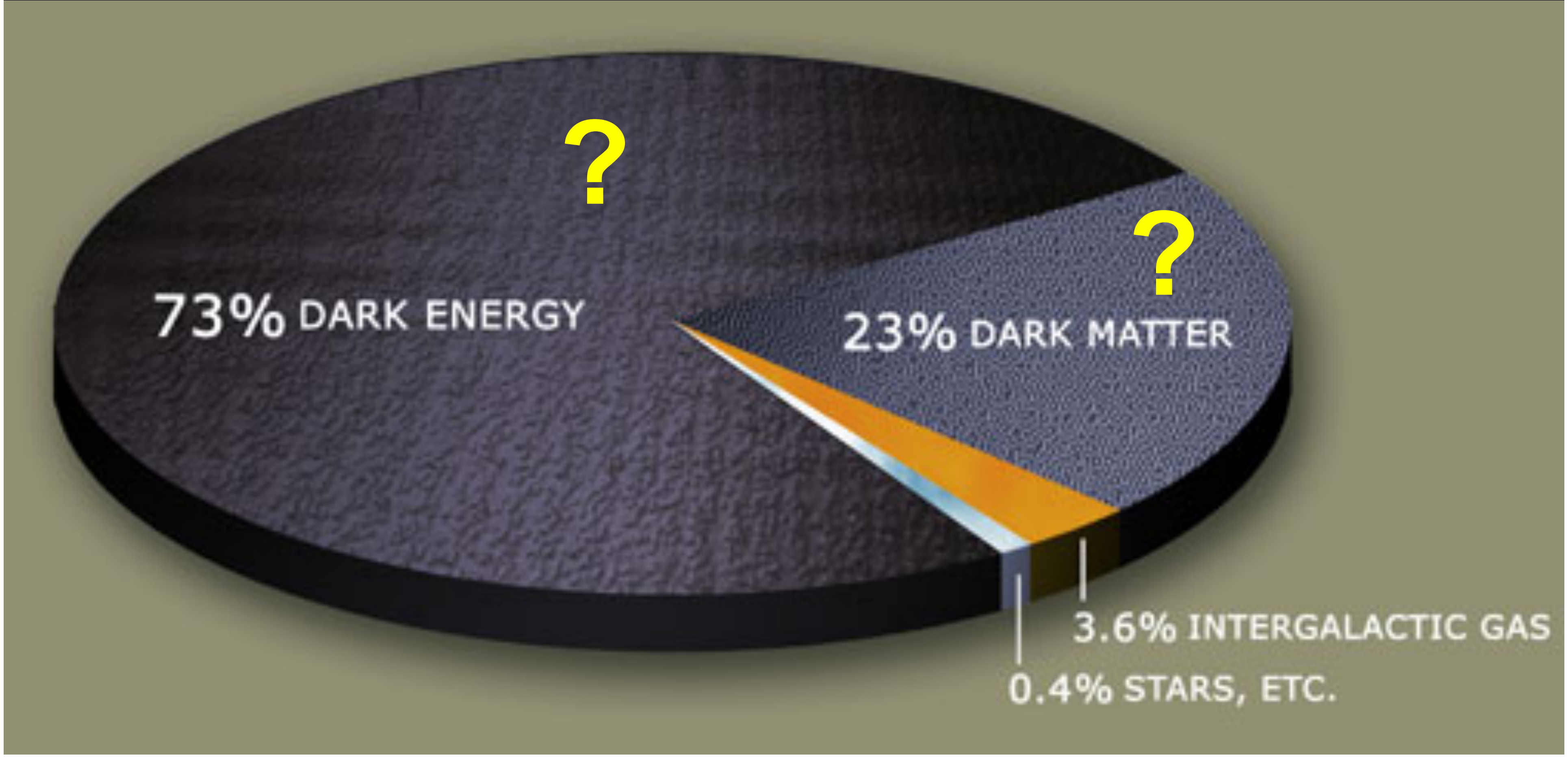

# Strange Situation in today Physics

- **Astronomy:** Data without Theory!
- **Quantum Gravity:** Theory without Data!

What is in the middle?

Dark Matter & Dark Energy?

# *Dark Energy is here to stay...*

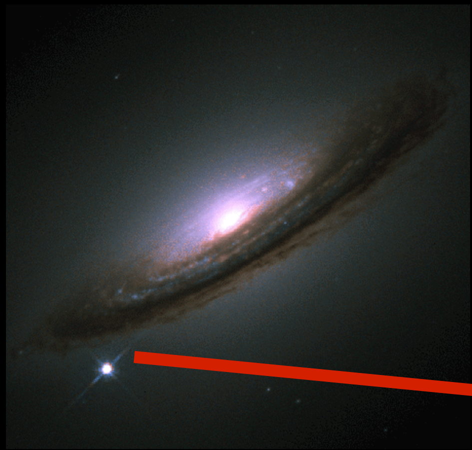

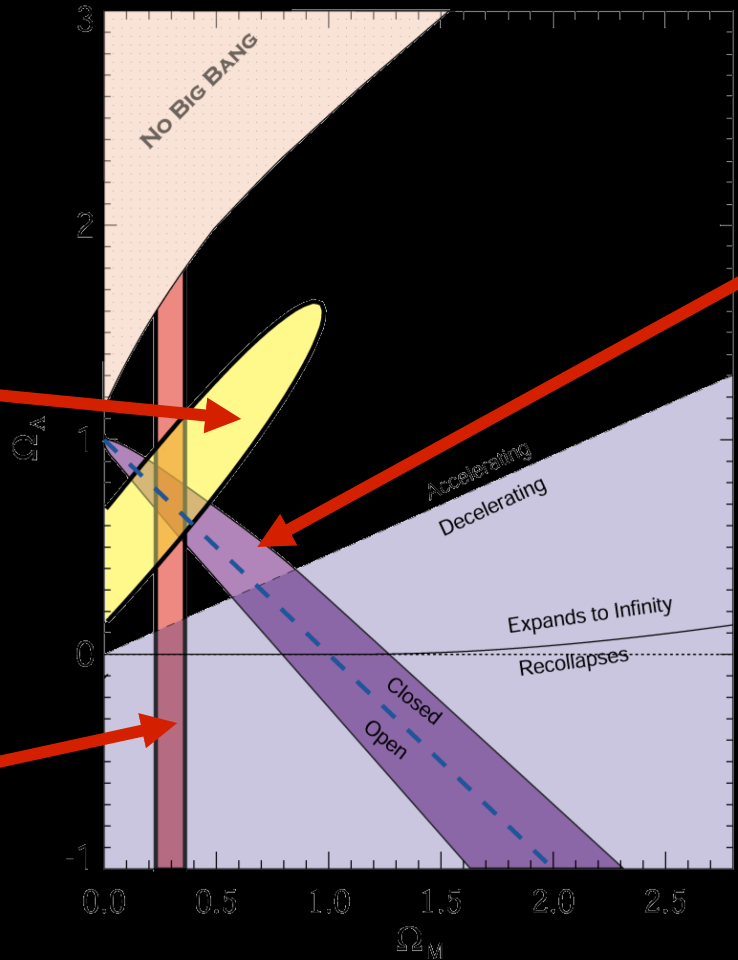


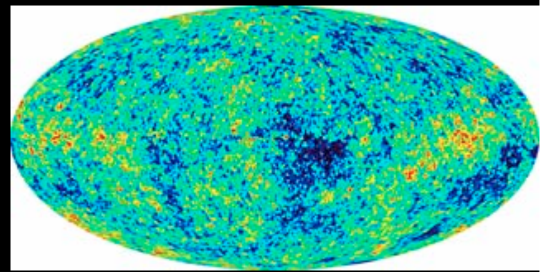

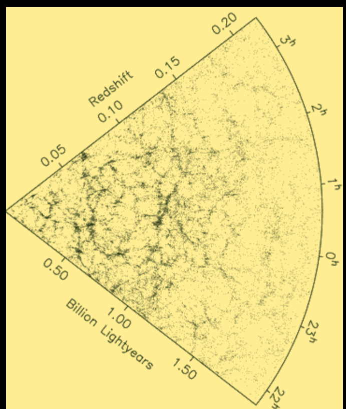


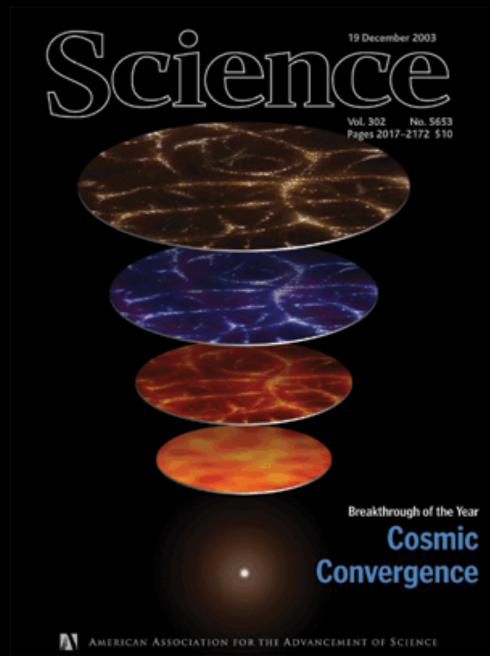

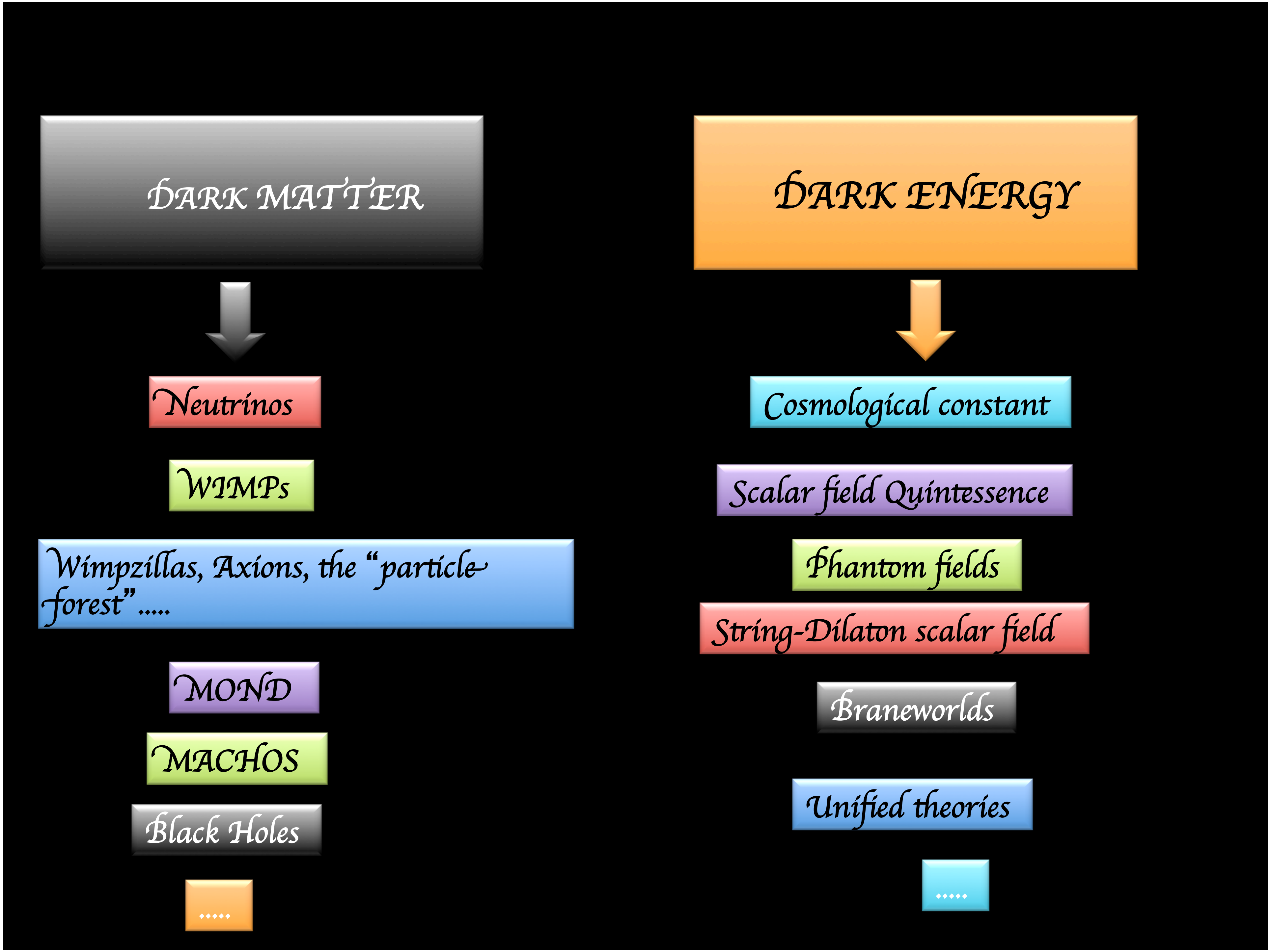
DARK MATTER
Neutrinos
WIMPs
Wimpzillas, Axions, the "particle forest".....
MOND
MACHOS
Black Holes
.....
DARK ENERGY
Cosmological constant
Scalar field Quintessence
Phantom fields
String-Dilaton scalar field
Braneworlds
Unified theories
.....

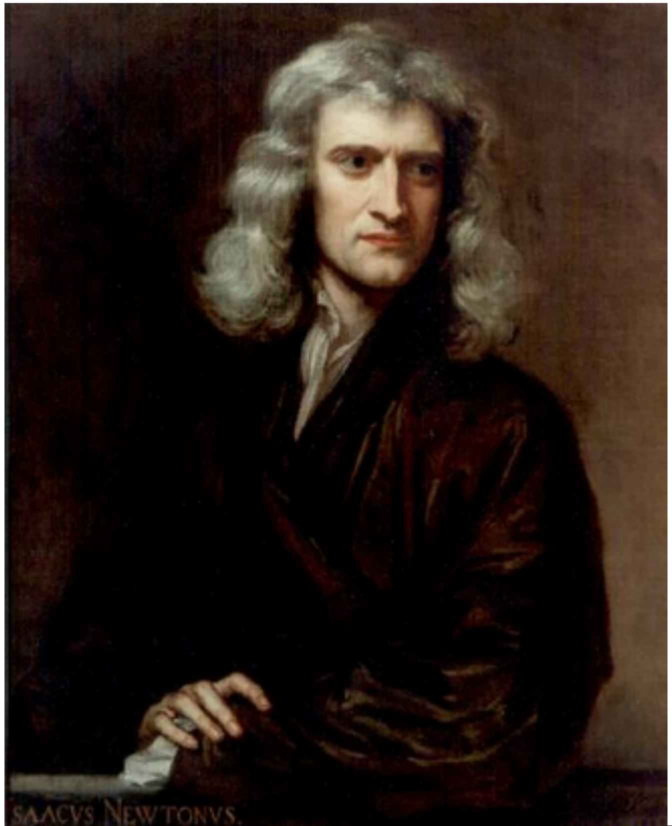


"…there are the ones that invent OCCULT FLUIDS to understand the Laws of Nature. They will come to conclusions, but they now run out into DREAMS and CHIMERAS neglecting the true constitution of things…..

…however there are those that from the simplest observation of Nature, they reproduce New Forces (i.e. New Theories)… "

From the Preface of PRINCIPIA (II Edition) 1687 by Isaac Newton, written by Mr. Roger Cotes

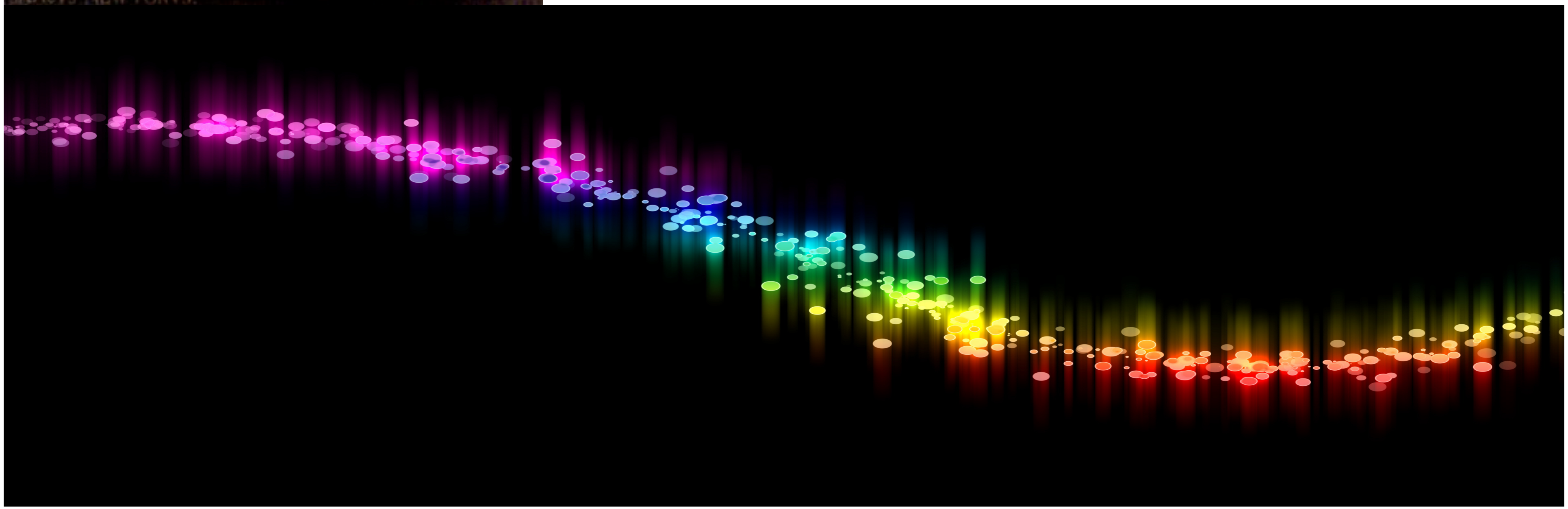

## There is a fundamental issue:

*Are extragalactic observations and cosmology probing the breakdown of General Relativity at large (IR) scales?*

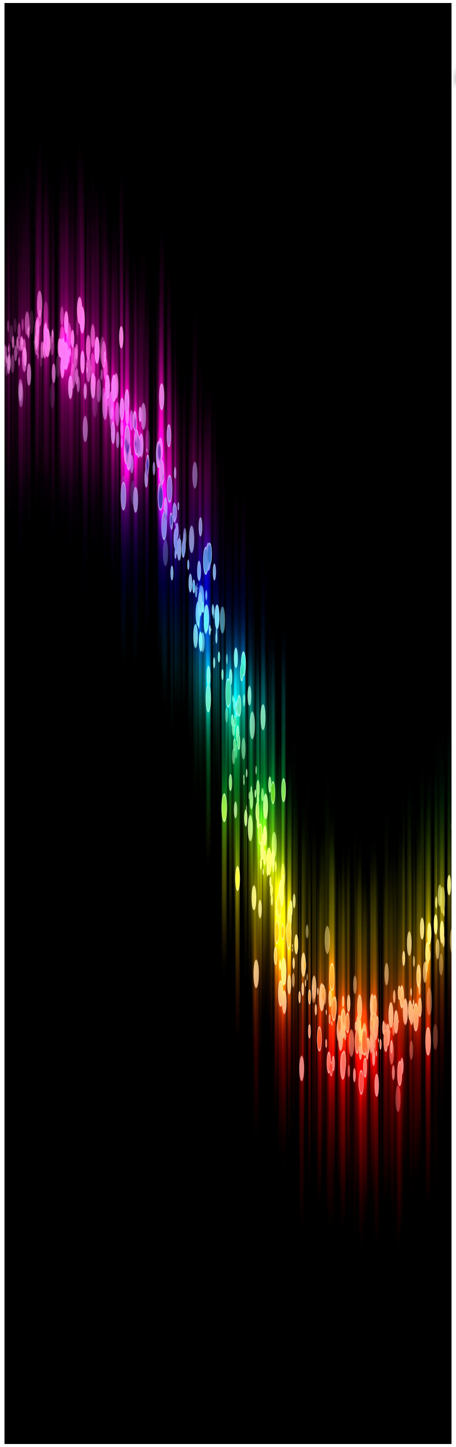

# The most important question in cosmology

How measuring the Universe?

Cosmological equations tell us that this question
is related to another question...

**Are there standard rulers, rods and clocks?**

The traditional way to search for solutions is the
cosmic distance ladder

| Method | Distance scale of validity | Average uncertainty |
|---|---|---|
| Zero point: GEOMETRICAL DISTANCE INDICATORS: THEIR OWN INTRINSIC UNCERTAINTY | | |
| Trigonometric parallax | 1 kpc | 0,1% a 1 pc, 100% a 1 kpc |
| Moving cluster | 1 kpc | 5% |
| Secular parallax | | |
| Statistical parallaxes | | |
| PRIMARY INDICATORS INTRINSIC UNCERTAINTY PLUS ZERO POINT INDICATORS CALIBRATION UNCERTAINTY | | |
| Main Sequence fit | ~50 pc – 50 kpc | 5% |
| RRLyrae | 1 Mpc | 1-5% |
| Cepheids | 25 Mpc | 5% |
| SECONDARY INDICATORS INTRINSIC UNCERTAINTY PLUS PREVIOUS TWO CALIBRATION UNCERTAINTIES | | |
| Type II SN (expading phtosphere method) | 100 Mpc | 20% (5% - 50%) |
| Most bright blue supergiants | 15 Mpc | 10% |
| Novae (MMRD method) | 20 Mpc | 20% (10% neighbour systems)) |
| Planetary Nebulae | 50 kpc – 20 Mpc | 5% |
| Fluctuations of the surface brightness | 5 kpc – 130 Mpc | 8% |
| Globular Clusters | 50 Mpc | 10% |
| Tully Fisher law | 10 – 500 Mpc | 15% |
| Fundamental plane | 10 – 250 Mpc | 5% |
| Brightest galaxy clusters | 10 – 200 Mpc | 20% |
| Type Ia SN | Up to ~ 8 Gpc | 5 – 15% |

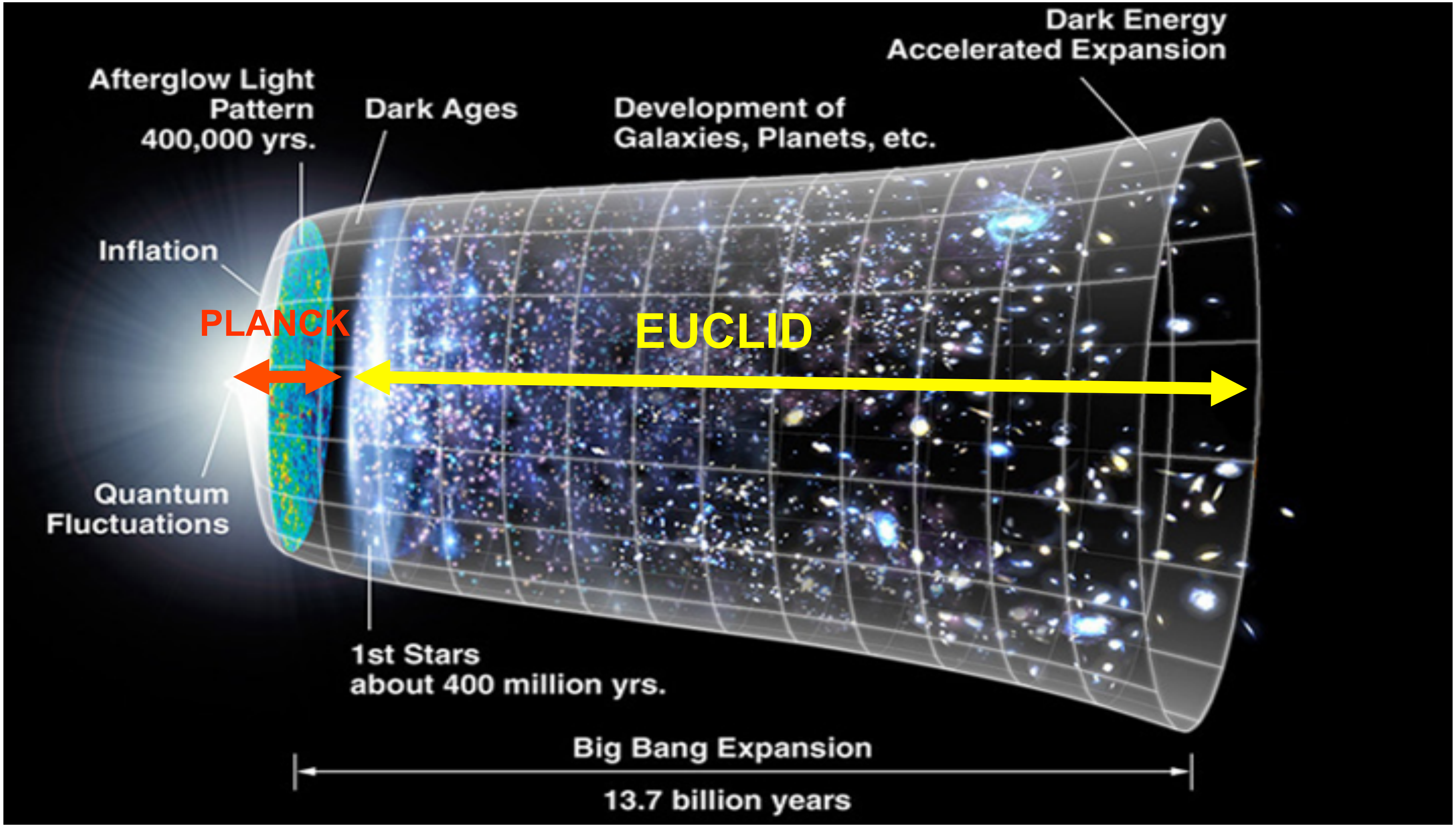


- *"The" high precision Dark Energy & Cosmology mission*
- *Essential and unbeatable synergy of imaging + spectroscopy*
- *Euclid will impact the whole astrophysics and cosmology for decades to come*

# SNeIa are powerful standard candles

SCP, HZT 1998

- ✓ hardly detectable at $z > 1.7$
- ✓ Degeneration in DE models
- ✓ Need of indicators at higher redshift

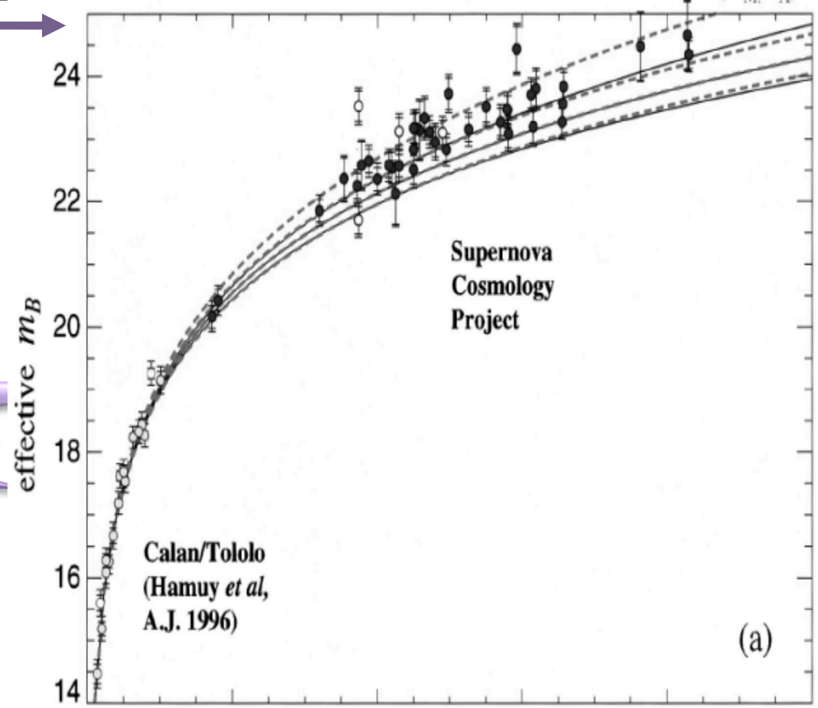


Possible solution: GRBs

- ✓ Most powerful explosions in the Universe
- ✓ Hints for structure formation
- ✓ Observed at considerable distances

→ Is it possible to frame them into the standard of cosmological distance ladder?

- ✓ Several models give account for GRB formation and dynamics e.g. (Meszaros, Piran 2006)...
- ✓ ...but none of them is intrinsically capable of connecting all the observable quantities !!
- ✓ …very flawed theory !
- ✓ currently GRBs cannot be used as standard candles
- ✓ however there are several observational correlations among photometric and spectral properties that could give cosmic distance indications.

# Properties of GRBs

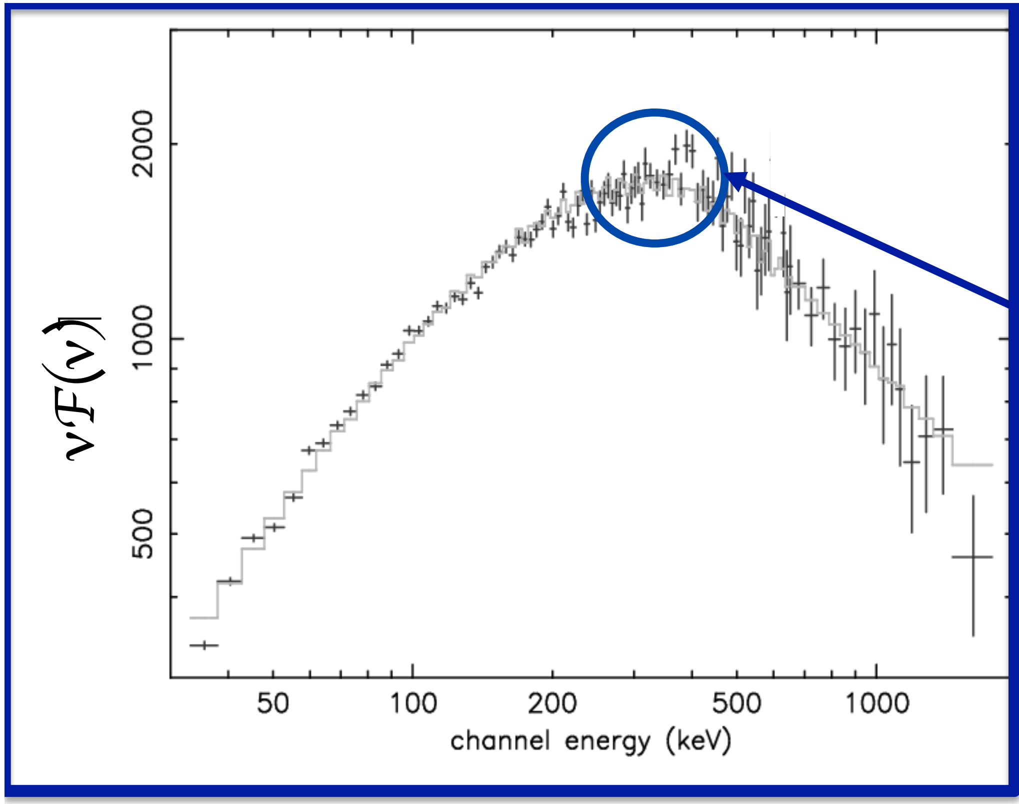


Peak Energy of the spectrum

Optical t-break

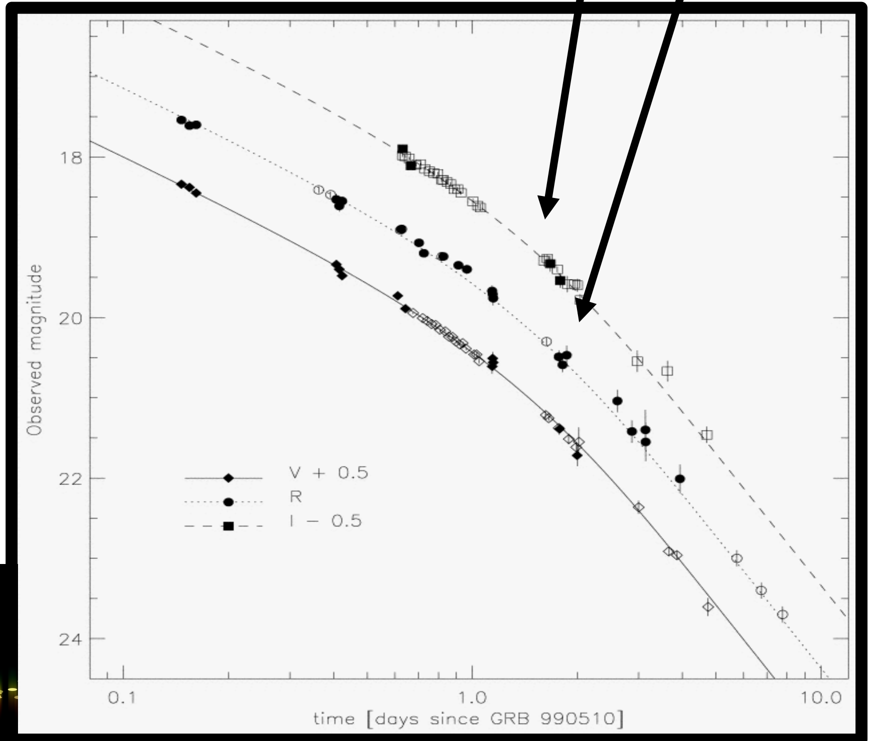


✓ E-iso is the isotropic energy emitted in the burst, while E-γ is the collimated E-iso

✓ The collimation angle is related to the optical t-break

# Peak energy – Isotropic energy Correlation

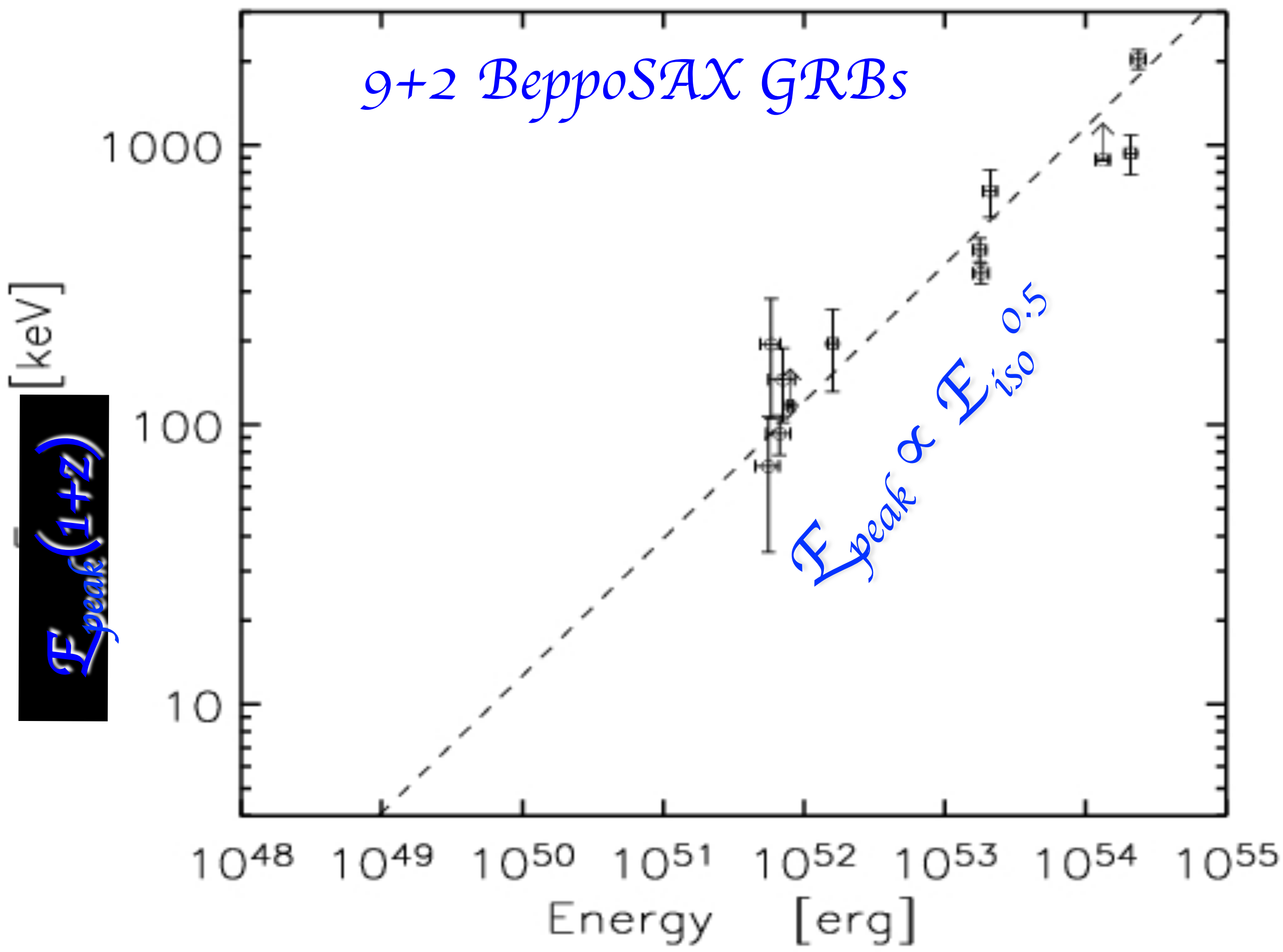


Amati et al. 2002

Nava et al. 2006; Ghirlanda et al. 2007

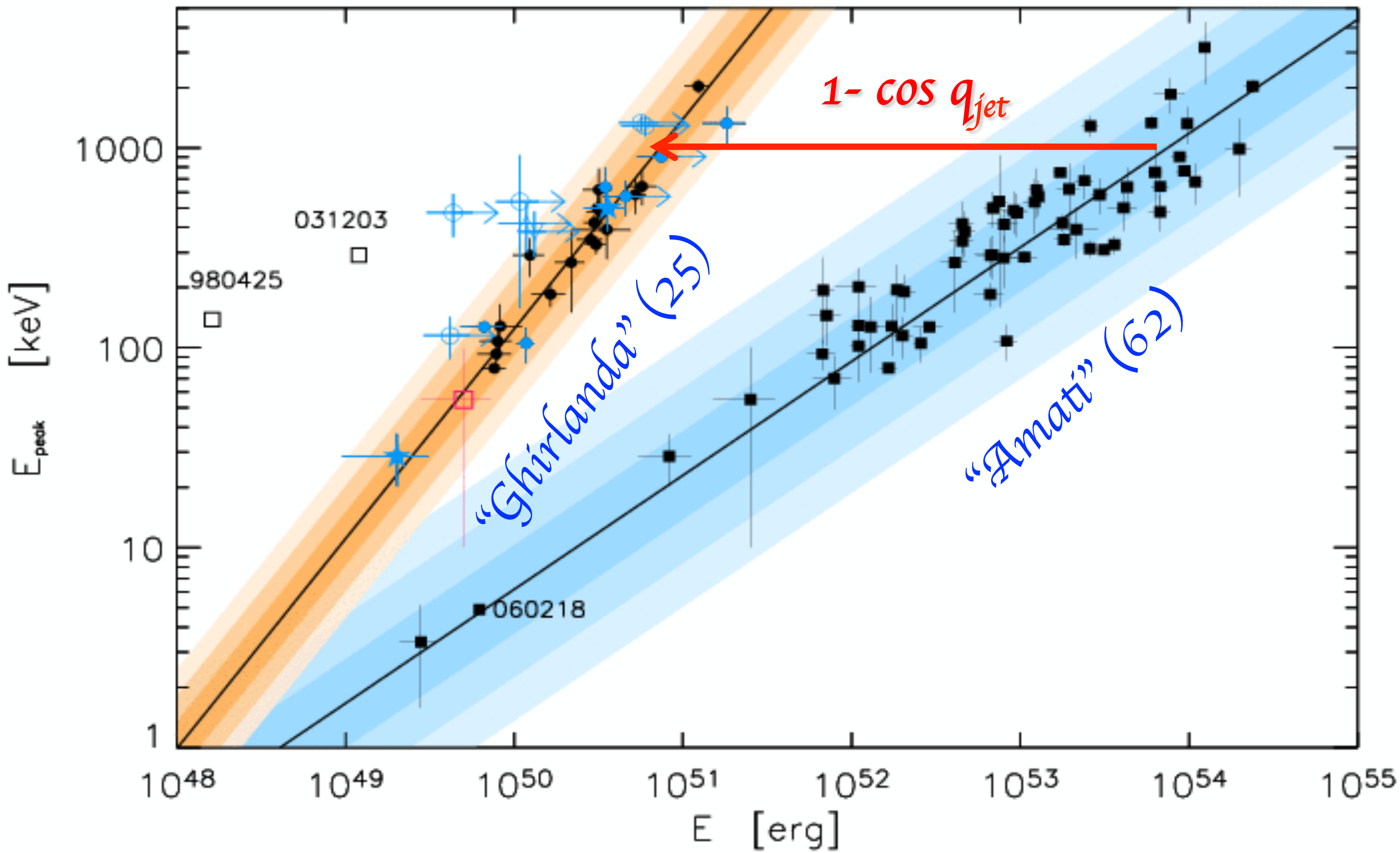

# Phenomenological model by SWIFT lightcurves

*A crucial point:*

•*a more complex behavior of the lightcurves, different from the broken power-law assumed in the past (Obrien et al. 2006,Sakamoto et al. 2007)*

*A significant step forward in determining common features in the afterglow*

•*X-ray afterglow lightcurves of the full sample of Swift GRBs shows that they may be fitted by the same analytical expression (Willingale et al. 2007)*

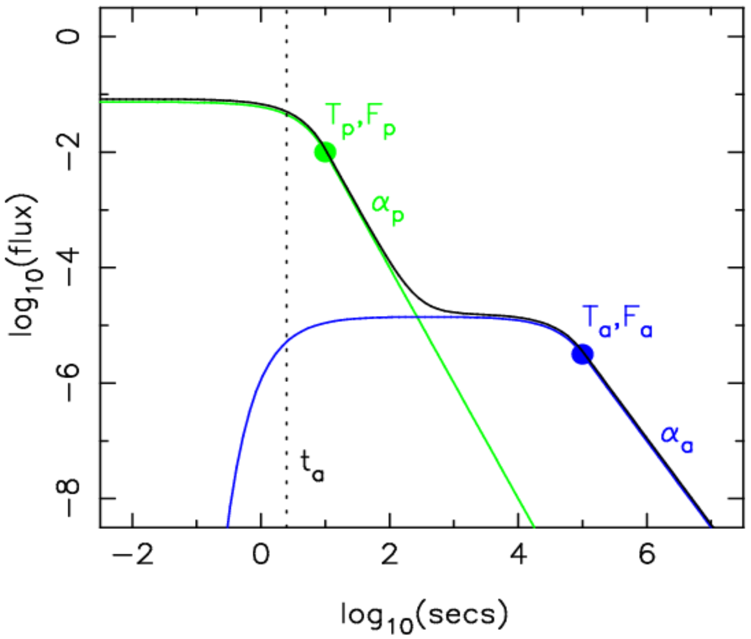


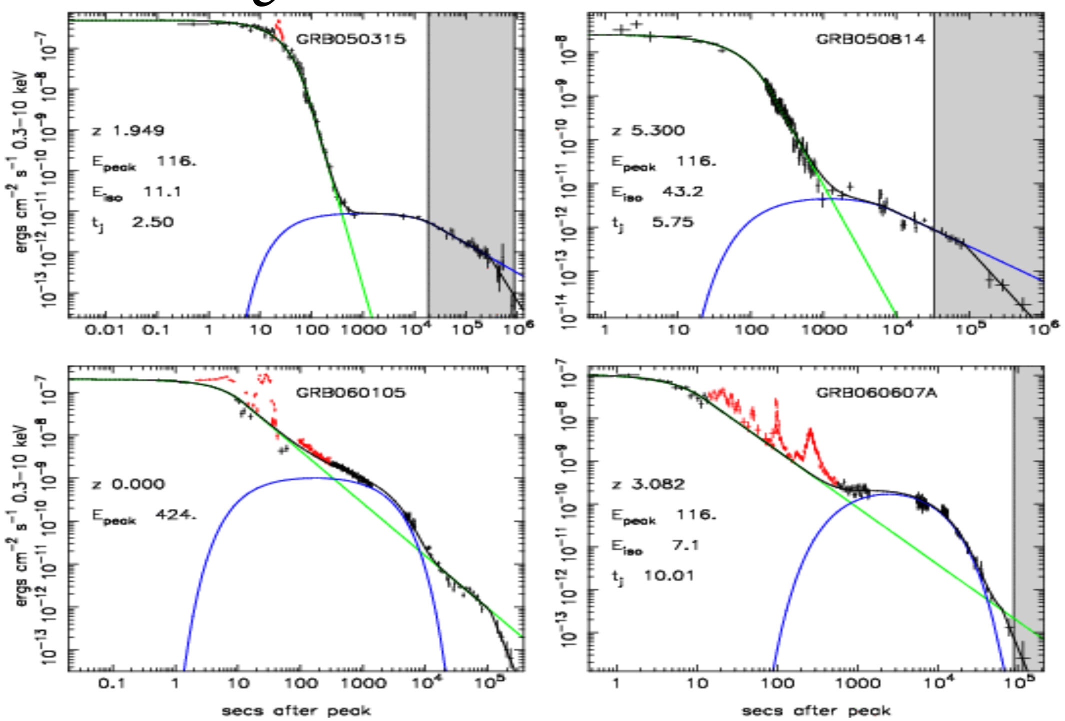

# A further correlation $L_X - T^*_a$

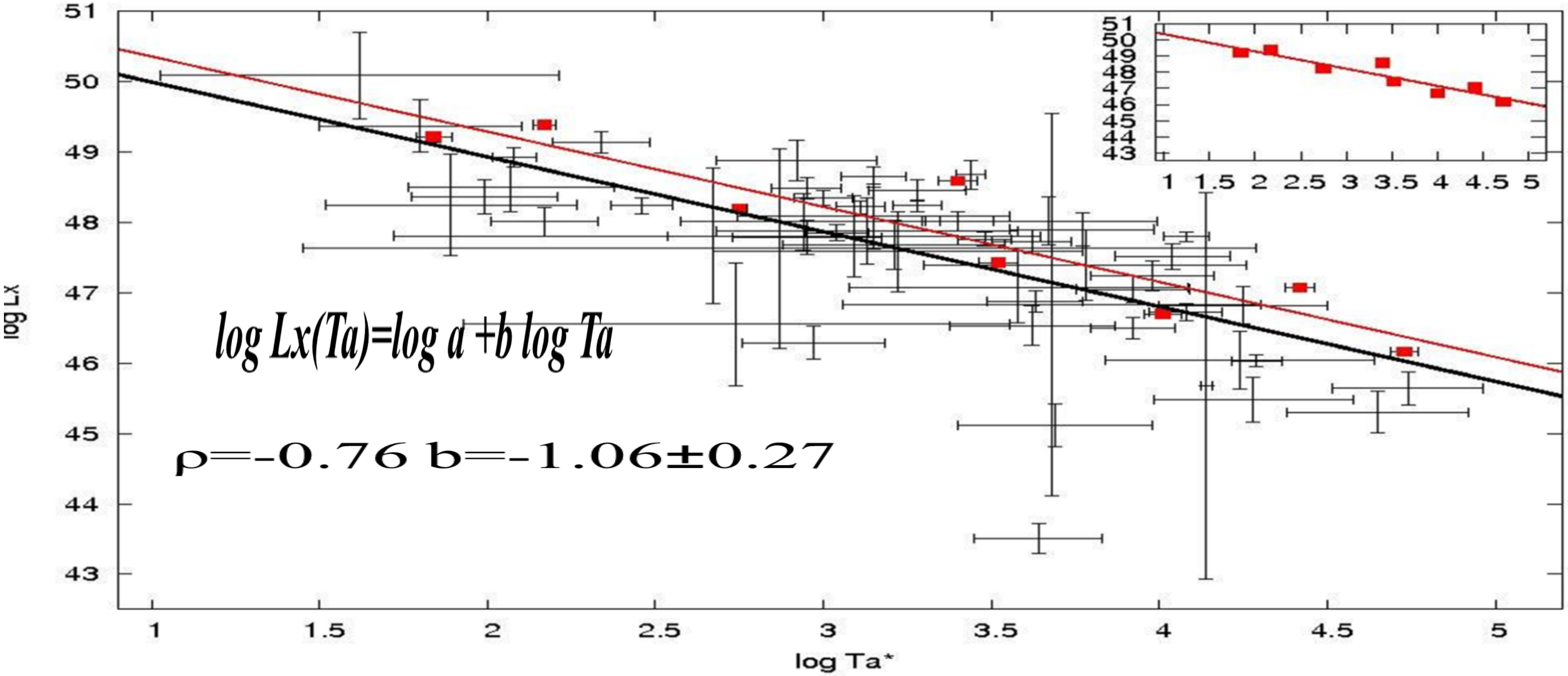


*Firstly discovered in 2008 by Dainotti, Cardone, & Capozziello MNRAS, 391, L 79D (2008)*

*Later uptdated by Dainotti, Willingale, Cardone, Capozziello & Ostrowski ApJL, 722, L 215 (2010)*

*$L_x(T^*_a)$ vs $T^*_a$ distribution for the sample of 62 long afterglows*

# Data and methodology

- Sample : 77 afterglows, 66 long, 11 from IC class (short GRBs with extended emission) detected by *Swift* from January 2005 up to March 2009, namely all the GRBs with good coverage of data that obey to the Willingale et al. 2007 model with firm redshift.

- Redshifts : from Greiner's web page http://www.mpe.mpg.de/jcg/grb.html.
- Redshift range 0.08 <z < 8.2
- Spectrum for each GRB was computed during the plateau (see Evans et al. 2010 web page http://www.swift.ac.uk/burst_analyser/)

For some GRBs in the sample, the error bars are so large that determination of the observables (Lx, Ta ) is not reliable. Therefore, we study effects of excluding such cases from the analysis (for details see Dainotti et al. 2011, ApJ 730, 135D ).

To study the low error subsamples we use the respective logarithmic error bars to formally define the error energy parameter

$$\sigma(E) = (\sigma_{Lx}^2 + \sigma_{Ta}^2)^{1/2}$$

# Prompt – afterglow correlations

Dainotti et al., MNRAS, 418,2202, 2011

A search for possible physical relations between
the afterglow characteristic luminosity $L^*_a \equiv L_x(T_a)$
and
the prompt emission quantities:

1.) the mean luminosity derived
as $\langle L^*_p \rangle_{45} = E_{iso}/T^*_{45}$

2.) $\langle L^*_p \rangle_{90} = E_{iso}/T^*_{90}$

3.) $\langle L^*_p \rangle_{T_p} = E_{iso}/T^*_p$

4.) the isotropic energy $E_{iso}$

# The search for standard GRBs continues

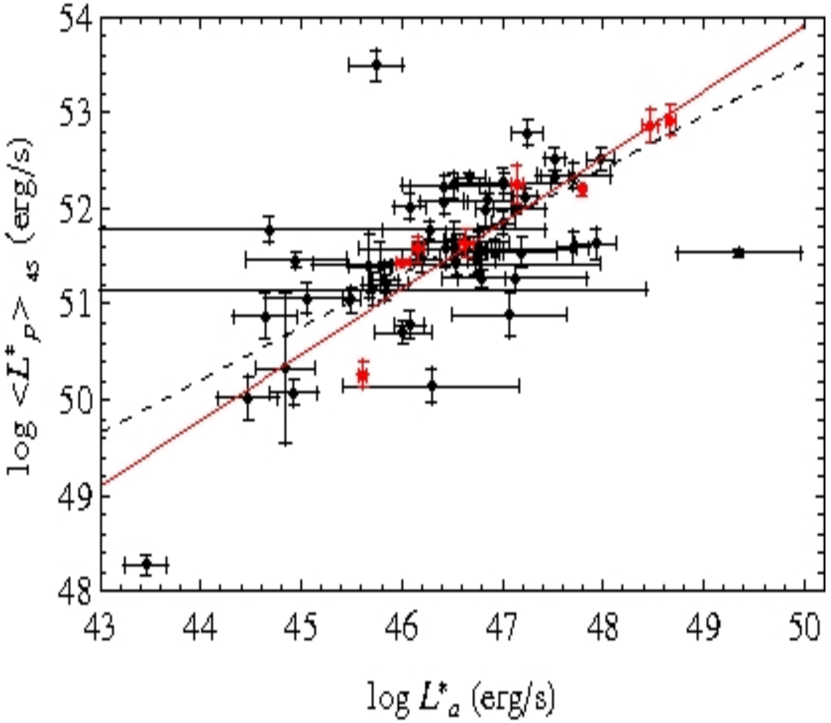


$L^*a$ vs. $<L^*p>45$ for 62 long GRBs
(the $\sigma$ (E) ≤ 4 subsample).

$$\sigma(E) = (\sigma_{Lx}^2 + \sigma_{Ta}^2)^{1/2}$$

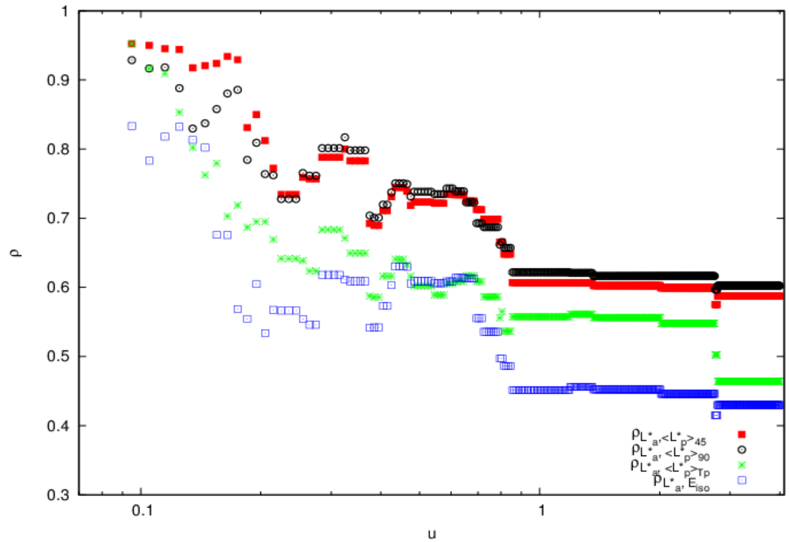


Correlation coefficients $\rho$ for for the long GRB subsamples
with the varying error parameter u

($L^*a$, $<L^*p>45$ ) - red
($L^*a$, $<L^*p>90$) - black
($L^*a$, $<L^*p>Tp$ ) - green
($L^*a$, Eiso ) - blue

# Updating the GRB Hubble diagram

- Allows to increase both the GRBs sample (83 GRBs vs 69) in Schaefer et al. 2006
- reduce the uncertainty on the distance moduli $\mu$ (z) of the

  14% Cardone, V.F., Capozziello, S. and Dainotti, M.G [2009, MNRAS, 400, 775C]

- The use of the HD with the Dainotti et al. correlation alone or in combination with other data shows that the use of GRBs leads to constraints in agreement with previous results in literature.
- A larger sample of high-luminosity GRBs can provide a valuable information in the search for the correct cosmological model

# Remark I

GRBs with well fitted afterglow light curves

obey tight physical scalings, both in their afterglow properties and in the prompt-afterglow relations.

We propose these GRBs as good candidates for

standardize Gamma Ray Burst

to be used both

- to construct GRB physical models
- for cosmological applications
- (Cardone, V.F., Capozziello, S. and Dainotti, M.G 2009, MNRAS, 400, 775C
- Cardone, V.F., Dainotti, M.G., Capozziello, S., and Willingale, R 2010, MNRAS, 408, 1181C)

# Division in redshift bins for the updated sample of 100 GRBs (with firm redshift and plateau emission)

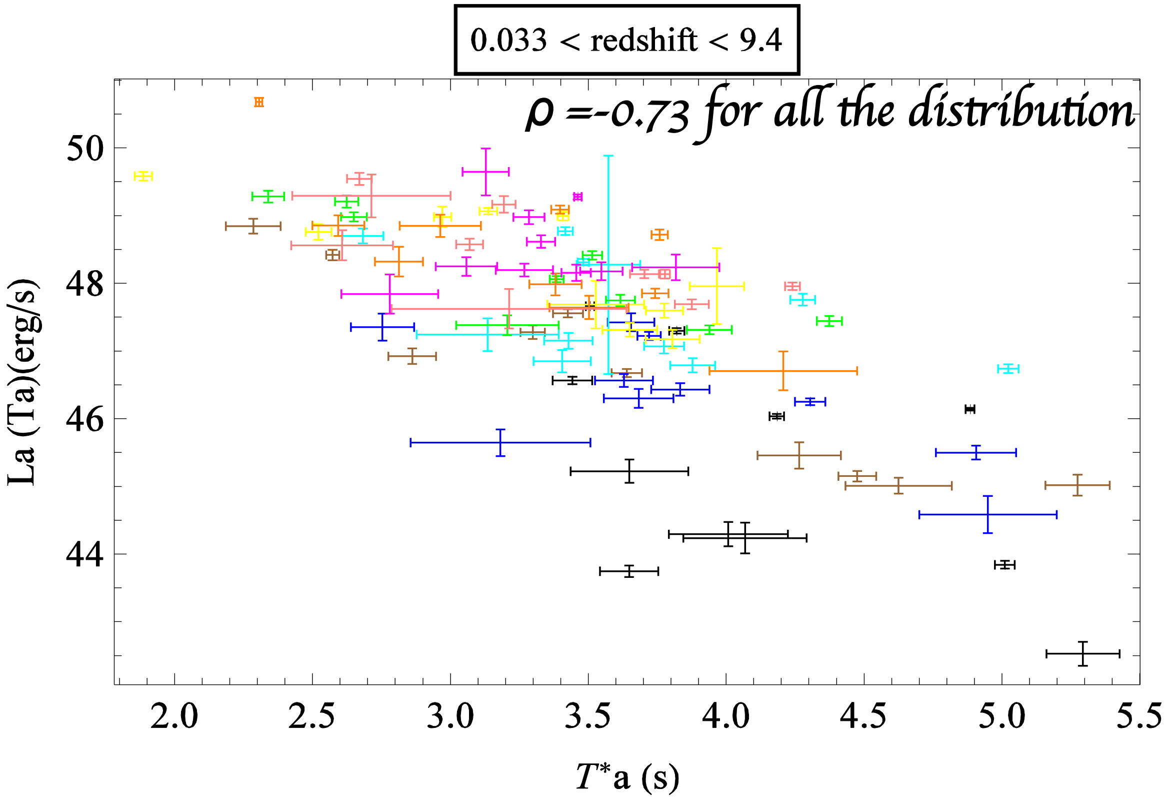


z< 0.69 Black

0.69 ≤ z < 1 Brown

1.49 ≤ z < 2.15 Cyan

2.15 ≤ z < 2.67 Yellow

2.47 ≤ z < 3.2 Green

3.2 ≤ z < 4.1 Pink

z ≥ 4.1 Red

*b= -1.62±0.20 1σ compatible with the previous fit*

*From a visual inspection it is hard to evaluate if there is a redshift induced correlation. Therefore, we have applied the test in Dainotti et al. 2011, ApJ, 730, 135D to check that the slope of every redshift bin is consistent with others. BUT It is not enough to answer definitely the question.*

# Luminosity vs 1+z

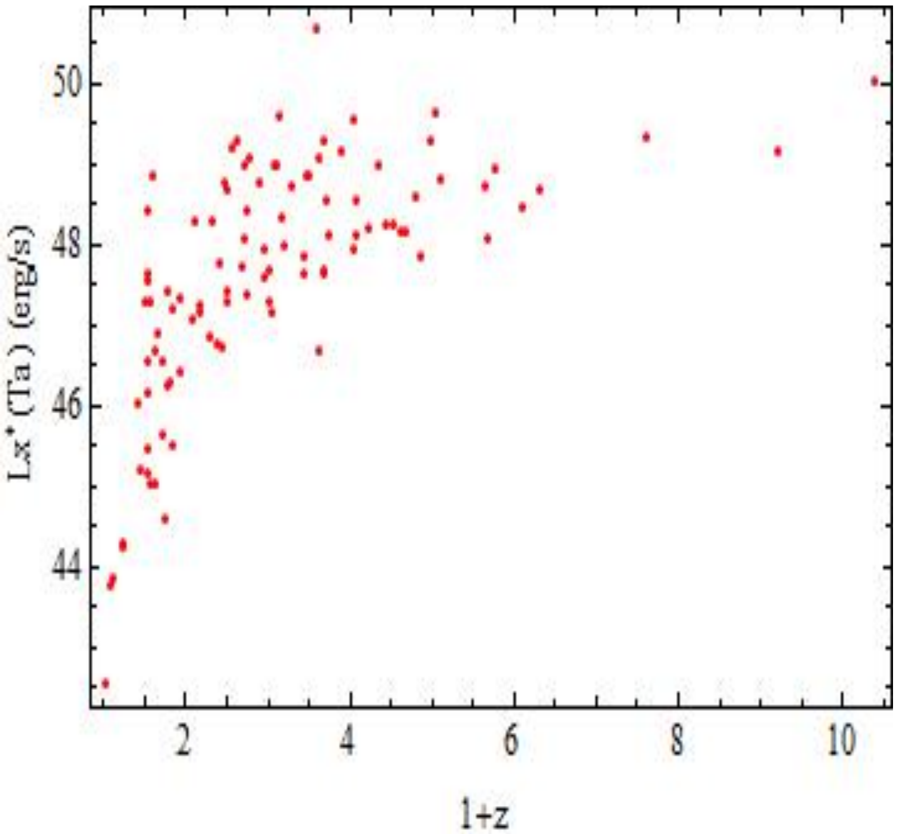


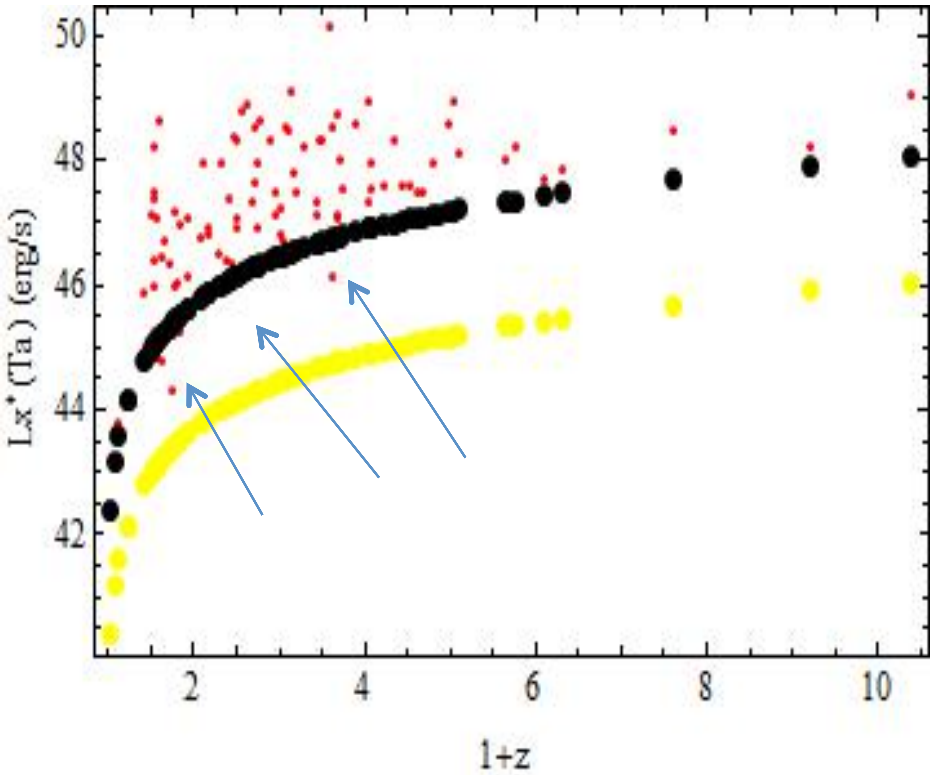


*The more appropriate Flux limit is the black dotted line Flux= 1.4 $\times 10^{-12}$*

*In such a way we have 90 GRBs in total, but with an appropriate limiting flux*

# Remark II

- The correlation La-Ta exists !!!
- It can be useful as model discriminator among several models that predict the Lx-Ta anti-correlation:
- energy injetion model from a spinning-down magnetar at the center of the fireball Dall' Osso et al. (2010), Xu & Huang (2011), Rowlinson & Obrien (2011).
- Accretion model onto the central engine as the long term powerhouse for the X-ray flux Cannizzo & Gerhels (2009), Cannizzo et al. 2010
- Prior emission model for the X-ray plateau Yamazaki (2009)
- and the phenomenological model by Ghisellini et al. (2009).
- For a correct cosmological use the unevolved observables are needed !!!!

# GRBs vs luminosity distance

$$L = 4\pi d_L^2(z) P_{bolo} \; ,$$

$$E_\gamma = 4\pi d_L^2(z) S_{bolo} F_{beam} (1+z)^{-1}$$

$$d_L(z) = \frac{c(1+z)}{H_0} \int_0^z \frac{dz'}{E(z')}$$

Circularity problem

We would like to use GRBs to probe cosmological models, but we need to adopt a cosmological model to get the GRBs Hubble diagram!

One can adopt 3 different strategies
to tackle this problem

1. *The simplest strategy is to assume a fiducial cosmological model, as the $\Lambda$CDM MODEL and determine its parameters by fitting, e.g., the SNeIa Hubble diagram. We set:*

$$\boxed{E^2(z) = \Omega_M(1+z)^3 + \Omega_\Lambda}$$

$$\boxed{\Omega_\Lambda = 1 - \Omega_M}$$

$$\boxed{(\Omega_M, h) = (0.261, 0.722)}$$

2. *Although the $\Lambda$CDM model fits remarkably well the data, it is worth stressing that a different cosmological model would give different values for $d_L(z)$ thus impacting the estimation of calibration parameters $(a, b, \sigma_{int})$*

*look for model indipendent approaches, e.g.:*

*COSMOGRAPHY*

$$(h, q_0, j_0, s_0, l_0) = (0.741, -0.56, 0.66, -0.41, 3.59)$$

3. *REGRESSION TECHNIQUE*

# The Hubble series

Connect the previous results with the Hubble series:

$$d_L(z) = \frac{cz}{H_0}\left\{1 + \frac{1}{2}[1-q_0]z - \frac{1}{6}\left[1 - q_0 - 3q_0^2 + j_0 + \frac{kc^2}{H_0^2 a_0^2}\right]z^2 + \frac{1}{24}\left[2 - 2q_0 - 15q_0^2 - 15q_0^3 + 5j_0 + 10q_0 j_0 + s_0 + \frac{2kc^2(1+3q_0)}{H_0^2 a_0^2}\right]z^3 + O(z^4)\right\}.$$

Where we have the cosmographic parameters

(Capozziello & Izzo A&A 2008)

$$H(t) = +\frac{1}{a}\frac{da}{dt},$$

$$j(t) = +\frac{1}{a}\frac{d^3a}{dt^3}\left[\frac{1}{a}\frac{da}{dt}\right]^{-3}$$

$$q(t) = -\frac{1}{a}\frac{d^2a}{dt^2}\left[\frac{1}{a}\frac{da}{dt}\right]^{-2}$$

$$s(t) = +\frac{1}{a}\frac{d^4a}{dt^4}\left[\frac{1}{a}\frac{da}{dt}\right]^{-4}$$

These parameters can be expressed in terms of the dark energy density and EoS.

$$w = p/\rho$$

CPL parametrization :

$$w(z)_{DE} = w_0 + w_a z\left(\frac{1}{1+z}\right)$$

$$E^2(z) = \Omega_M(1+z)^3 + \Omega_X(1+z)^{3(1+w_0+w_a)}e^{-\frac{3w_a z}{1+z}},$$

$$E(z) = H/H_0$$

We can evaluate the cosmographic parameters

$$q_0 = \frac{1}{2} + \frac{3}{2}(1-\Omega_M)w_0\,,$$

$$j_0 = 1 + \frac{3}{2}(1-\Omega_M)\left[3w_0(1+w_0) + w_a\right]$$

$$\begin{aligned} s_0 \;=\; & -\frac{7}{2} - \frac{33}{4}(1-\Omega_M)w_a \\ & - \frac{9}{4}(1-\Omega_M)\left[9 + (7-\Omega_M)w_a\right]w_0 \\ & - \frac{9}{4}(1-\Omega_M)(16-3\Omega_M)w_0^2 \\ & - \frac{27}{4}(1-\Omega_M)(3-\Omega_M)w_0^3\,. \end{aligned}$$

# Building up the Hubble diagram

Let us calculate $d_l$ for each GRB → $d_l = \left(\frac{E_{iso}}{4\pi S'_{bolo}}\right)^{\frac{1}{2}}$

Where $S'_{bolo} = S_{bolo}/(1+z)$

so we obtain

1) $$d_l = \left[\frac{10^a \left(\frac{E_p(1+z)}{300keV}\right)^{b_1} \left(\frac{t_b}{(1+z)1day}\right)^{b_2}}{4\pi S'_{bolo}}\right]^{1/2}$$

2) $$d_l = 7.575 \frac{(1+z)a^{2/3}[E_p(1+z)/100\,\mathrm{keV}]^{2b/3}}{(S_{bolo}t_b)^{1/2}(n_0\eta_\gamma)^{1/6}}\mathrm{Mpc.}$$

# Examples of cosmography by GRBs

- ✓ *Liang-Zhang relation (Liang & Zhang 2005) :*

$$\log E_{iso} = a + b_1 \log \frac{E_p(1+z)}{300keV} + b_2 \log \frac{t_b}{(1+z)1day}$$

- ✓ *Ghirlanda relation (Ghirlanda et al 2004) :*

$$\log E_\gamma = a + b \log \frac{E_p}{300keV}$$

*Where*

$$E_\gamma = (1 - \cos\theta_{jet})E_{iso} \qquad \theta_{jet} = 0.163\left(\frac{t_b}{1+z}\right)^{3/8}\left(\frac{n_0\eta_\gamma}{E_{iso,52}}\right)^{1/8}$$

# GRB data fitting

- Estimates of the deceleration, jerk and snap parameters
- Degeneration in jerk $j_0 + 1 + \frac{kd_H^2}{a_0^2}$ eliminated for k = 0

Flat Universe

- Two different fits :

1) $$d(z) = \sum_{i=1}^{3} a_i z^i$$

2) $$\ln[d(z)/(zMpc)] = \sum_{i=1}^{3} b_i z^i$$

Constraints:
(Komatsu et al 2008)

$H_0 \simeq 70 \pm 2$ km/sec/Mpc

$\Lambda$CDM-universe $(w_0, w_a) = (-1, 0)$

# 2D empirical correlations for luminosity distance

Consider the general case of two observable quantities (x; y) related by a power - law relation which, in a log - log plane, reads

$\boxed{\log y = a \log x + b}$ Setting $\boxed{y = \kappa d_L^2(z)}$ one can then estimate the distance modulus as

$$\boxed{\mu = 25 + 5 \log d_L(z) = 25 + (5/2)(a \log x + b - \log \kappa)}$$

1. $\boxed{L\text{ - }E_{peak}}$ $y = L$ $x = E_{peak}(1+z)/300$
2. $\boxed{L\text{ - }\tau_{lag}}$ $y = L$ $x = \tau_{lag}(1+z)^{-1}/0.1$
3. $\boxed{L\text{ - }\tau_{RT}}$ $y = L$ $x = \tau_{RT}(1+z)^{-1}/0.1$
4. $\boxed{L\text{ - }V}$ $y = L$ $x = V(1+z)/0.02$
5. $\boxed{E_\gamma\text{ - }E_{peak}}$ $y = E_\gamma$ $x = E_{peak}(1+z)/300$
6. $\boxed{E_{iso}\text{ - }E_{peak}}$ $E_{iso} = E_\gamma / F_{beam}$ $x = E_{peak}(1+z)/300$

$$\boxed{\begin{array}{l} L = 4\pi d_L^2(z) P_{bolo} \;, \\ E_\gamma = 4\pi d_L^2(z) S_{bolo} F_{beam} (1+z)^{-1} \end{array}}$$

# Calibration parameters

While the $X$ quantities are directly observed for each GRBs, the determination of $Y$ (either the luminosity $L$ or the collimated energy $E_\gamma$) needs for object's luminosity distance.

The three methods allow us to get three different values for $Y$ so that it is worth investigating whether this fact has some significant impact on the calibration parameters ($a$, $b$, $\sigma_{int}$) for the correlations of interest.

| Id | $\mathcal{N}$ | $\chi^2/d.o.f.$ | $(a, b, \sigma_{int})_{bf}$ | $a$ | $b$ | $\sigma_{int}$ |
|---|---|---|---|---|---|---|
| $L$ - $E_{peak}$ | 39 | 1.05 | (1.05, 49.75, 0.46) | $0.99^{+0.21\ +0.41}_{-0.22\ -0.43}$ | $49.61^{+0.64\ +1.14}_{-0.21\ -0.97}$ | $0.46^{+0.08\ +0.16}_{-0.05\ -0.11}$ |
| $L$ - $E_{peak}$ | 39 | 1.04 | (1.06, 49.66, 0.47) | $1.02^{+0.21\ +0.44}_{-0.20\ -0.43}$ | $49.53^{+0.57\ +1.15}_{-0.10\ -0.71}$ | $0.47^{+0.07\ +0.15}_{-0.05\ -0.10}$ |
| $L$ - $E_{peak}$ | 39 | 1.08 | (0.95, 50.00, 0.43) | $0.84^{+0.23\ +0.47}_{-0.23\ -0.44}$ | $50.02^{+0.68\ +1.24}_{-0.21\ -0.72}$ | $0.45^{+0.05\ +0.17}_{-0.07\ -0.12}$ |
| $L$ - $\tau_{lag}$ | 27 | 1.07 | (-0.70, 51.60, 0.47) | $-0.65^{+0.17\ +0.36}_{-0.16\ -0.31}$ | $51.60^{+0.12\ +0.25}_{-0.05\ -0.17}$ | $0.48^{+0.06\ +0.19}_{-0.06\ -0.11}$ |
| $L$ - $\tau_{lag}$ | 27 | 1.09 | (-0.68, 51.57, 0.47) | $-0.64^{+0.14\ +0.28}_{-0.15\ -0.33}$ | $51.60^{+0.07\ +0.17}_{-0.08\ -0.21}$ | $0.49^{+0.08\ +0.20}_{-0.07\ -0.13}$ |
| $L$ - $\tau_{lag}$ | 27 | 1.09 | (-0.67, 51.67, 0.43) | $-0.62^{+0.15\ +0.27}_{-0.14\ -0.33}$ | $51.70^{+0.10\ +0.18}_{-0.07\ -0.18}$ | $0.44^{+0.07\ +0.16}_{-0.06\ -0.12}$ |
| $L$ - $\tau_{RT}$ | 31 | 1.16 | (-1.09, 51.81, 0.45) | $-1.02^{+0.24\ +0.46}_{-0.19\ -0.47}$ | $51.82^{+0.05\ +0.12}_{-0.04\ -0.10}$ | $0.46^{+0.08\ +0.20}_{-0.06\ -0.11}$ |
| $L$ - $\tau_{RT}$ | 31 | 1.20 | (-1.03, 51.78, 0.46) | $-0.92^{+0.25\ +0.47}_{-0.24\ -0.49}$ | $51.83^{+0.04\ +0.10}_{-0.07\ -0.15}$ | $0.48^{+0.08\ +0.18}_{-0.07\ -0.13}$ |
| $L$ - $\tau_{RT}$ | 31 | 1.10 | (-1.07, 51.88, 0.40) | $-0.97^{+0.22\ +0.45}_{-0.22\ -0.47}$ | $51.88^{+0.07\ +0.14}_{-0.02\ -0.10}$ | $0.41^{+0.07\ +0.15}_{-0.06\ -0.11}$ |
| $L$ - $V$ | 37 | 1.10 | (0.34, 52.60, 0.61) | $0.33^{+0.18\ +0.43}_{-0.20\ -0.52}$ | $52.53^{+0.25\ +0.56}_{-0.16\ -0.47}$ | $0.62^{+0.10\ +0.20}_{-0.07\ -0.14}$ |
| $L$ - $V$ | 37 | 1.09 | (0.40, 52.65, 0.61) | $0.37^{+0.21\ +0.49}_{-0.25\ -0.50}$ | $52.66^{+0.16\ +0.54}_{-0.30\ -0.69}$ | $0.63^{+0.09\ +0.23}_{-0.08\ -0.14}$ |
| $L$ - $V$ | 37 | 1.10 | (0.37, 52.73, 0.56) | $0.33^{+0.19\ +0.41}_{-0.22\ -0.52}$ | $52.64^{+0.24\ +0.52}_{-0.22\ -0.61}$ | $0.57^{+0.09\ +0.13}_{-0.07\ -0.13}$ |
| $E_\gamma$ - $E_{peak}$ | 14 | 1.17 | (1.77, 46.71, 0.17) | $1.71^{+0.22\ +0.44}_{-0.24\ -0.65}$ | $47.01^{+0.23\ +1.01}_{-0.58\ -1.09}$ | $0.20^{+0.07\ +0.19}_{-0.06\ -0.10}$ |
| $E_\gamma$ - $E_{peak}$ | 14 | 1.21 | (1.71, 46.80, 0.18) | $1.62^{+0.24\ +0.51}_{-0.29\ -0.64}$ | $47.28^{+0.27\ +1.10}_{-0.71\ -1.35}$ | $0.21^{+0.07\ +0.16}_{-0.06\ -0.11}$ |
| $E_\gamma$ - $E_{peak}$ | 14 | 1.16 | (1.72, 46.81, 0.17) | $1.66^{+0.26\ +0.55}_{-0.28\ -0.57}$ | $47.16^{+0.38\ +0.95}_{-0.66\ -1.31}$ | $0.20^{+0.07\ +0.18}_{-0.07\ -0.14}$ |
| $E_{iso}$ - $E_{peak}$ | 40 | 0.79 | (1.58, 49.16, 0.52) | $1.54^{+0.27\ +0.55}_{-0.26\ -0.50}$ | $49.26^{+0.45\ +1.03}_{-0.45\ -1.04}$ | $0.51^{+0.09\ +0.21}_{-0.07\ -0.13}$ |
| $E_{iso}$ - $E_{peak}$ | 40 | 0.81 | (1.24, 49.57, 0.52) | $1.00^{+0.37\ +0.75}_{-0.33\ -0.62}$ | $50.16^{+0.99\ +1.69}_{-0.30\ -1.27}$ | $0.52^{+0.11\ +0.24}_{-0.08\ -0.16}$ |
| $E_{iso}$ - $E_{peak}$ | 40 | 0.79 | (1.22, 50.03, 0.51) | $1.04^{+0.35\ +0.73}_{-0.38\ -0.70}$ | $50.09^{+0.97\ +1.77}_{-0.27\ -1.26}$ | $0.52^{+0.12\ +0.27}_{-0.08\ -0.15}$ |

# Evolution with redshift

$\log y = a \log x + b$

*The calibration parameters ($a$, $b$, $\sigma_{int}$) evolve with the redshift ?*

*To investigate this issue, we consider two different possibilities for the evolution with z*

**1.** $Y = \alpha \log(1+z) + aX + b$

| Id | $\chi^2/d.o.f.$ | $(a, b, \alpha, \sigma_{int})_{bf}$ | $a$ | $b$ | $\alpha$ | $\sigma_{int}$ |
|---|---|---|---|---|---|---|
| $L$ - $E_{peak}$ | 1.08 | (0.89, 50.77, 0.67, 0.41) | $0.82^{+0.20}_{-0.19}$ | $50.75^{+0.59}_{-0.65}$ | $0.68^{+0.18}_{-0.30}$ | $0.44^{+0.06}_{-0.06}$ |
| $L$ - $\tau_{lag}$ | 1.10 | (-0.58, 50.38, 0.88, 0.39) | $-0.57^{+0.12}_{-0.14}$ | $50.39^{+0.66}_{-0.58}$ | $0.87^{+0.30}_{-0.33}$ | $0.41^{+0.07}_{-0.06}$ |
| $L$ - $\tau_{RT}$ | 1.16 | (-0.79, 51.22, 0.65, 0.44) | $-0.64^{+0.21}_{-0.25}$ | $50.97^{+0.70}_{-0.75}$ | $0.76^{+0.36}_{-0.33}$ | $0.47^{+0.07}_{-0.06}$ |
| $L$ - $V$ | 1.23 | (-0.10, 50.27, 1.07, 0.54) | $-0.05^{+0.26}_{-0.37}$ | $50.29^{+0.91}_{-0.96}$ | $1.04^{+0.52}_{-0.50}$ | $0.57^{+0.11}_{-0.08}$ |
| $E_\gamma$ - $E_{peak}$ | 1.37 | (1.57, 50.64, 0.00, 0.14) | $1.48^{+0.23}_{-0.26}$ | $50.42^{+0.51}_{-0.57}$ | $0.13^{+0.31}_{-0.28}$ | $0.20^{+0.07}_{-0.06}$ |
| $E_{iso}$ - $E_{peak}$ | 0.81 | (1.39, 51.58, 0.58, 0.48) | $1.29^{+0.28}_{-0.28}$ | $51.57^{+0.84}_{-0.81}$ | $0.58^{+0.44}_{-0.45}$ | $0.50^{+0.10}_{-0.08}$ |

**2.** $Y = (a_0 + a_1 z)X + (b_0 + b_1 z)$

| Id | $\chi^2/d.o.f.$ | $(a_0, \log a_1, b_0, \log b_1, \sigma_{int})_{bf}$ | $a_0$ | $\log a_1$ | $b_0$ | $\log b_1$ | $\sigma_{int}$ |
|---|---|---|---|---|---|---|---|
| $L$ - $E_{peak}$ | 1.12 | (0.89, -2.69, 51.49, -0.21, 0.41) | $0.89^{+0.22}_{-0.25}$ | $-3.05^{+2.13}_{-3.63}$ | $51.87^{+0.19}_{-0.46}$ | $-0.78^{+0.64}_{-3.06}$ | $0.44^{+0.03}_{-0.05}$ |
| $L$ - $\tau_{lag}$ | 1.13 | (-0.60, -4.43, 51.31, -0.07, 0.40) | $-0.64^{+0.16}_{-0.19}$ | $-2.78^{+1.61}_{-2.85}$ | $51.61^{+0.49}_{-0.45}$ | $-0.28^{+0.27}_{-2.83}$ | $0.43^{+0.08}_{-0.06}$ |
| $L$ - $\tau_{RT}$ | 1.17 | (-1.56, -0.08, 52.38, -0.70, 0.44) | $-0.95^{+0.33}_{-0.46}$ | $-1.81^{+1.59}_{-3.90}$ | $52.42^{+0.19}_{-0.53}$ | $-1.81^{+1.60}_{-3.91}$ | $0.47^{+0.07}_{-0.06}$ |
| $L$ - $V$ | 1.36 | (-0.15, -2.16, 51.40, 0.03, 0.52) | $-0.10^{+0.41}_{-0.44}$ | $-1.79^{+1.49}_{-4.81}$ | $51.85^{+0.39}_{-0.53}$ | $-0.77^{+0.76}_{-2.86}$ | $0.58^{+0.10}_{-0.08}$ |
| $E_\gamma$ - $E_{peak}$ | 1.70 | (0.79, 0.04, 50.37, -0.56, 0.10) | $1.40^{+0.23}_{-0.47}$ | $-1.70^{+1.63}_{-2.67}$ | $50.61^{+0.08}_{-0.15}$ | $-2.86^{+1.91}_{-3.84}$ | $0.17^{+0.08}_{-0.06}$ |
| $E_{iso}$ - $E_{peak}$ | 0.79 | (0.94, -0.23, 52.00, -0.15, 0.49) | $1.27^{+0.33}_{-0.50}$ | $-1.78^{+1.61}_{-2.54}$ | $52.56^{+0.16}_{-0.34}$ | $-1.73^{+1.42}_{-2.41}$ | $0.50^{+0.10}_{-0.08}$ |

# GRBs Hubble diagram

Once the calibration parameters for a given Y-X correlation have been obtained, it is then possible to estimate the distance modulus of a given GRB by the measured value of X. Indeed, for a given Y, the luminosity distance is:

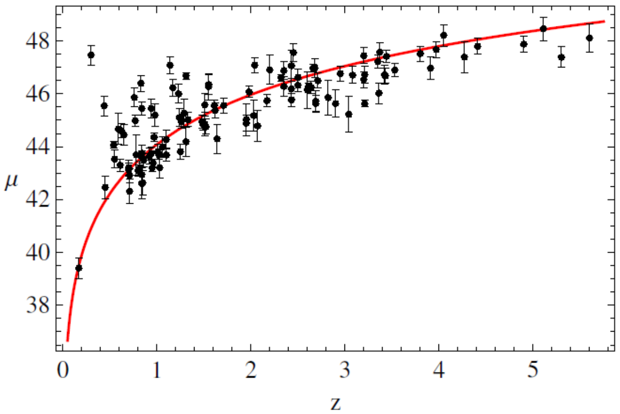


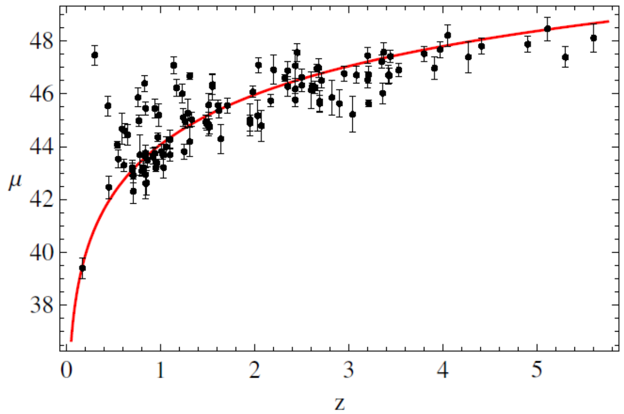


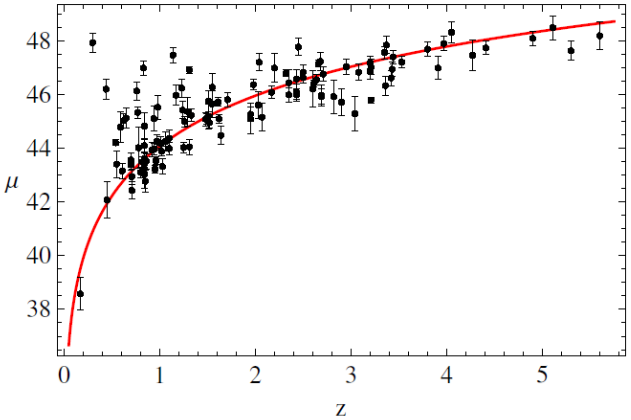


It is possible to both reduce the uncertainties and (partially) wash out the hidden systematic errors by averaging over the different correlations available for a given GRB

(Cardone, Capozziello, Perillo MNRAS 2011).

# Updating the GRB Hubble diagram

We add the $L_X$ - $T_a$ correlation with $T_a$ the X-ray luminosity at the time $T_a$ and $T_a$ a timescale characterizing the late afterglow decay. The use of this new correlation allows to increase both the GRBs sample and reduce the uncertainty on $\mu(z)$.

| Id | $\mathcal{N}$ | $(a, b, \sigma_{int})_{ML}$ | $\delta_{med}$ | $\delta_{rms}$ | $\mathcal{C}(\delta, z)$ | $a^{+1\sigma\ +2\sigma}_{-1\sigma\ -2\sigma}$ | $(\sigma_{int})^{+1\sigma\ +2\sigma}_{-1\sigma\ -2\sigma}$ |
|---|---|---|---|---|---|---|---|
| $E_\gamma$ - $E_p$ | 27 | (1.38, 50.56, 0.25) | 0.01 | 0.38 | -0.17 | $1.37^{+0.23\ +0.48}_{-0.26\ -0.30}$ | $0.30^{+0.11\ +0.28}_{-0.09\ -0.16}$ |
| $L$ - $E_p$ | 64 | (1.24, 52.16, 0.45) | -0.05 | 0.51 | 0.07 | $1.24^{+0.18\ +0.36}_{-0.18\ -0.36}$ | $0.48^{+0.07\ +0.17}_{-0.07\ -0.12}$ |
| $L$ - $\tau_{lag}$ | 38 | (-0.80, 52.28, 0.37) | 0.02 | 0.40 | 0.40 | $-0.80^{+0.14\ +0.30}_{-0.14\ -0.30}$ | $0.40^{+0.09\ +0.21}_{-0.07\ -0.12}$ |
| $L$ - $\tau_{RT}$ | 62 | (-0.89, 52.48, 0.44) | 0.04 | 0.47 | 0.27 | $-0.89^{+0.16\ +0.31}_{-0.18\ -0.38}$ | $0.46^{+0.07\ +0.16}_{-0.06\ -0.11}$ |
| $L$ - $V$ | 51 | (1.03, 52.49, 0.48) | -0.09 | 0.50 | 0.25 | $1.04^{+0.39\ +0.60}_{-0.29\ -0.57}$ | $0.51^{+0.09\ +0.21}_{-0.07\ -0.13}$ |
| $L_X$ - $T_a$ | 28 | (-0.58, 48.09, 0.33) | -0.12 | 0.43 | -0.21 | $-0.58^{+0.18\ +0.38}_{-0.18\ -0.37}$ | $0.39^{+0.14\ +0.33}_{-0.11\ -0.20}$ |

$$l_L(z) = \begin{cases} E_\gamma (1+z)/4\pi F_{beam} S_{bolo} \\ L/4\pi P_{bolo} \\ L_X (1+z)^{\beta_a + 2}/4\pi F_X(T_a) \end{cases}$$

$\cancel{E_{iso} - E_{peak}}$

Joining the Willingale et al. (2007) and Schaefer (2007) samples and considering that 17 objects are in common, we end up with a catalogo of 83 GRBs which we used to build the Hubble diagram assuming a $\Lambda$CDM concordance cosmology. The $L_X$ - $T_a$ correlation does not introduce any bias.

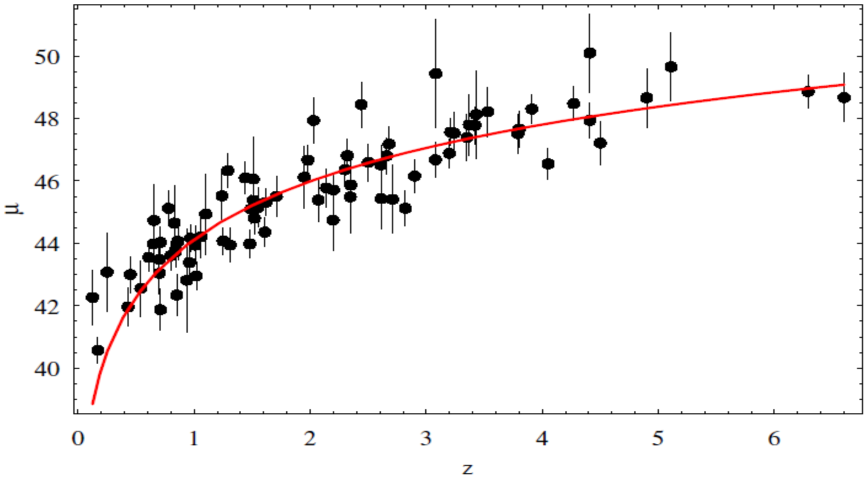


*Varying the cosmological model:* although not preferred by the data, a varying equation of state (EoS) for the dark energy fluid is still a viable (and theoretically better motivated) option. A large class of dark energy models predict a depedence of the EoS on the scale factor a which is well fitted by the *Chevallier -Polarski – Linder (CPL) ansatz* (Chevallier & Polarski 2001; Linder 2003) :

$$w(a) = w_0 + w_a(1-a) = w_0 + w_a z/(1+z)$$

$$E^2(z) = \Omega_M(1+z)^3 + \Omega_X(1+z)^{3(1+w_0+w_a)} e^{-\frac{3w_a z}{1+z}} \qquad \Omega_X = 1 - \Omega_M$$

*Changing the cosmological model used for the calibration has such a small impact on the estimated μ (z) and so on the final Hubble diagram.*

# Cosmographic Results

- CPL parameterization works for the total matter-energy density.
- Results agree with the ΛCDM model.
- Transition epoch from deceleration to acceleration ($z \approx 5$ )
- Presence of a phantom regime at present epoch ( $z << 1$ )
- Need for a new parametrization of EoS more general than CPL?
- Need for wide GRB samples, in particular GRBs at high
- redshift ( $z \geq 6$ ).
- Could the used relations be hints towards a GRB standard
- model?

# Summary and perspectives

- GRBs are promising candidates to expand the Hubble diagram up to very high z, complementing SNeIa.
- As the Phillips law is the basic tool to standardize SNeIa, the hunt for a similar relation to be used for GRBs has lead to different empirically motivated 2D scaling relations.
- Circularity problem could be avoided using e.g. Amati relation!!
- Three different methods to estimate the luminosity distance: 1) a fiducial $\Lambda$CDM model, 2) cosmography, 3) local regression.
- We find that this three conceptually different methods to estimate the luminosity distance and hence calibrate the GRBs scaling relations lead to consistent results

- A redshift evolution of GRB scaling relation has to be taken into account.
- Cosmography suggests that GRBs are distance rulers (it is premature the statement "distance indicators" as for SNeIa).
- Matching with other distance indicators like SNeIa, clusters, giant ellipticals and CMBR, one could achieve a robust cosmic distance ladder at any redshift.
- Improving the relation between GRBs observables to understand physical mechanisms (a GRB physical model from cosmology??)
- $H(z)$ is a powerful tool to discriminate among degenerate DE cosmological models ( $\Lambda$CDM, $f(R)$, quintessence, etc..) see Diaferio et al. 2011.
- Degeneration could be removed at high redshift

*Work in progress!!!*